Ann Nucl Med (2009) 23:301–309
DOI 10.1007/s12149-009-0240-x

ORIGINAL ARTICLE

Preclinical and the first clinical studies on [^{11}C]CHIBA-1001 for mapping α7 nicotinic receptors by positron emission tomography

Jun Toyohara · Muneyuki Sakata · Jin Wu · Masatomo Ishikawa · Keiichi Oda · Kenji Ishii · Masaomi Iyo · Kenji Hashimoto · Kiichi Ishiwata

Received: 30 October 2008 / Accepted: 29 December 2008 / Published online: 1 April 2009

Abstract
Objective 4-[^{11}C]methylphenyl 2,5-diazabicyclo[3.2.2] nonane-2-carboxylate ([^{11}C]CHIBA-1001), a 4-methyl-substituted derivative of the selective α7 nicotinic acetylcholine receptor (α7 nAChR) partial agonist 4-bromophenyl 1,4 diazabicyclo[3.2.2]nonane-4-carboxylate (SSR180711), is a potential radioligand for mapping α7 nAChRs in the brain by positron emission tomography (PET). In this study, we performed preclinical and first clinical PET studies using [^{11}C]CHIBA-1001 for imaging α7 nAChRs in the human brain.
Methods [^{11}C]CHIBA-1001 was synthesized by methylation of the tributylstannyl precursor with [^{11}C]CH_3I in a palladium-promoted Stille cross-coupling reaction. The radiation absorbed-dose of [^{11}C]CHIBA-1001 in humans was calculated from distribution data in mice. The acute toxicity of CHIBA-1001 at a dose of 3.20 mg/kg body weight, which is more than 41,000-fold the clinical equivalent dose of [^{11}C]CHIBA-1001, was evaluated. The mutagenicity of CHIBA-1001 was studied by a reverse mutation test in *Salmonella typhimurium* (Ames test). Metabolite analysis in the mouse brain was carried out by high-performance liquid chromatography. The first clinical PET imaging of α7 nAChRs with [^{11}C]CHIBA-1001 in a normal volunteer was also performed.
Results A suitable preparation method for [^{11}C]CHIBA-1001 injection was established. The radiation absorbed-dose by [^{11}C]CHIBA-1001 in humans was low enough for clinical use, and no acute toxicity or mutagenicity of CHIBA-1001 was found. Most radioactivity in the mouse brain was detected as an unchanged form, although peripherally [^{11}C]CHIBA-1001 was degraded. We successfully performed brain imaging by PET with [^{11}C]CHIBA-1001 in a normal volunteer. A 90-min dynamic scan showed a rapid accumulation and gradual washout of radioactivity in the brain. The highest distribution volume of [^{11}C]CHIBA-1001 was found in the thalamus; however, regional differences in brain radioactivity were small. Peripherally, [^{11}C]CHIBA-1001 was stable in humans: >80% of the radioactivity in plasma was detected as the unchanged form for 60 min.
Conclusions These results demonstrate that [^{11}C]CHIBA-1001 is a suitable radioligand to use in clinical trials for imaging α7 nAChRs in the human brain, providing acceptable dosimetry and pharmacological safety at the dose required for adequate PET imaging.

Keywords α7 Nicotinic receptor · [^{11}C]CHIBA-1001 · Central nervous system · Positron emission tomography

J. Toyohara · M. Sakata · J. Wu · M. Ishikawa · K. Oda · K. Ishii · K. Ishiwata (✉)
Positron Medical Center, Tokyo Metropolitan Institute of Gerontology, 35-2 Sakaecho, Itabashi-ku, Tokyo 173-0015, Japan
e-mail: ishiwata@pet.tmig.or.jp

J. Toyohara · J. Wu · K. Hashimoto
Division of Clinical Neuroscience, Chiba University Center for Forensic Mental Health, Chiba, Japan

M. Ishikawa · M. Iyo
Department of Psychiatry, Chiba University Graduate School of Medicine, Chiba, Japan

Introduction

NEURONAL nicotinic acetylcholine receptors (nAChRs) are ubiquitously distributed in the human brain and consist of various combinations of α1–α10 and β2–β4 subunits [1]. Among the several nAChRs subtypes present in the central

nervous system (CNS), the homomeric α7 and heteromeric α4β2 subtypes of nAChRs are predominant in the brain [2]. These subtypes are best characterized in terms of ligand selectivity, as they can be studied by means of binding techniques: [^{3}H]cytisine or [^{3}H]nicotine can label α4β2 nAChRs, and [^{125}I]α-bungarotoxin or [^{3}H]methyllycaconitine ([^{3}H]MLA) is used to label α7 nAChRs [3]. In the rat brain, high densities of α7 nAChRs are found in the hippocampus, hypothalamus, and cortical areas, whereas they are expressed to lesser degrees in the striatum and cerebellum [4]. Although the distribution of α7 nAChRs in primates is still not completely known, the available data suggest that it does not differ greatly, overall, from that in rodents. However, there are some discrepancies: [^{125}I]α-bungarotoxin binding and α7 mRNA expression are more diffuse in monkey brain than in rodent brain [5, 6]. α7 nAChRs are most dense in the thalamic nuclei, with moderate to low densities in the hippocampus, prefrontal cortex, caudate, putamen, and substantia nigra [5]. Human postmortem brain studies showed that α7 nAChRs are present in the thalamic nuclei and moderately dense in the hippocampus, cortex, and cerebellum [7, 8]. The α7 nAChRs modulate neurotransmitter release presynaptically and generate excitatory responses postsynaptically [9]. In addition, the receptors present in perisynaptic locations modulate other inputs to the neuron [9]. Furthermore, α7 nAChRs are involved in sensory gating, memory, and neuronal plasticity. A number of studies suggest that α7 nAChRs play an important role in the pathologic states of several neurological and psychiatric disorders, such as Alzheimer's disease, dementia with Lewy bodies, and schizophrenia [10–14].

On the basis of these backgrounds, several researchers have developed radiotracers for selective imaging of the α7 nAChRs in the human brain by positron emission tomography (PET) and single-photon emission computed tomography (SPECT) [15–17]. Despite these efforts, there have been no clinical studies using radioligands for α7 nAChRs in the human brain. Very recently, Hashimoto et al. [18] developed 4-[^{11}C]methylphenyl 2,5-diazabicyclo[3.2.2]nonane-2-carboxylate ([^{11}C]CHIBA-1001) as a novel PET ligand for α7 nAChRs in the conscious monkey brain. An in vitro binding study showed that the IC_{50} value of CHIBA-1001 for [^{125}I]α-bungarotoxin binding to the rat brain homogenates was 45.8 nM. Also, CHIBA-1001 (1 or 10 μM) was found to have less activity (inhibition lower than 50%) for a 28-standard receptor binding profile. [^{11}C]CHIBA-1001 distribution in the monkey brain measured by PET was consistent with the regional distribution of α7 nAChRs. Moreover, brain uptake of [^{11}C]CHIBA-1001 was dose-dependently blocked by pretreatment with the selective α7 nAChR agonist SSR180711, but was not altered by the selective α4β2 nAChR agonist A-85380 [18]. These findings prompted us to undertake a preclinical study of [^{11}C]CHIBA-1001.

In this study, we established a suitable method for preparing clinical [^{11}C]CHIBA-1001 injections. We also calculated the radiation dosimetry of [^{11}C]CHIBA-1001 for humans from a distribution study in mice and examined the acute toxicity and mutagenicity of CHIBA-1001 in a preclinical study. Because the previous study did not examine whether the labeled metabolites of [^{11}C]CHIBA-1001 were present in the monkey brain [18], we investigated in this study the possibility of the presence of the labeled metabolite in the brain using mice. Finally, we demonstrated the first clinical PET imaging of α7 nAChRs with [^{11}C]CHIBA-1001 in a healthy subject.

Materials and methods

General

CHIBA-1001 and its precursor, 4-(tributylstannyl)phenyl 2,5-diazabicyclo[3.2.2]nonane-2-carboxylate, was prepared by a previously described method [18]. All chemical reagents were obtained from commercial sources. Male ddY mice were obtained from Tokyo Laboratory Animals Co., Ltd (Tokyo, Japan). The animal studies were approved by the Animal Care and Use Committee of the Tokyo Metropolitan Institute of Gerontology and Chiba University. The clinical study of [^{11}C]CHIBA-1001 was also approved by the Ethics Committees of the Tokyo Metropolitan Institute of Gerontology and Chiba University Graduate School of Medicine. Written informed consent was obtained from each subject after the procedures had been fully explained.

Radiosynthesis

Carbon methylation of the precursor via a palladium-mediated Stille cross-coupling reaction with [^{11}C]methyl iodide was performed by adapting a previously described procedure with a slight modification (Fig. 1) [19]. [^{11}C]CO_2 was produced by the proton irradiation of nitrogen gas at 25 μA for 30–55 min using the CYPRIS 370 cyclotron (Sumitomo Heavy Industries Ltd, Tokyo, Japan). [^{11}C]Methyl iodide was produced from [^{11}C]CO_2 with an automated system (Sumitomo Heavy Industries, Tokyo, Japan). A solution of tri(*o*-tolyl)phosphine (3.7 mg, 12 μmol) in *N,N*-dimethylformamide (DMF) (0.15 ml) and the precursor in DMF (0.1 ml, 1.0 mg/ml) was prepared. Immediately before the end of irradiation, it was added to the dry septum-equipped vial containing a mixture of copper chloride (1.2 mg, 12 μmol), potassium carbonate (1.7 mg, 12 μmol), and tris(dibenzylideneacetone)

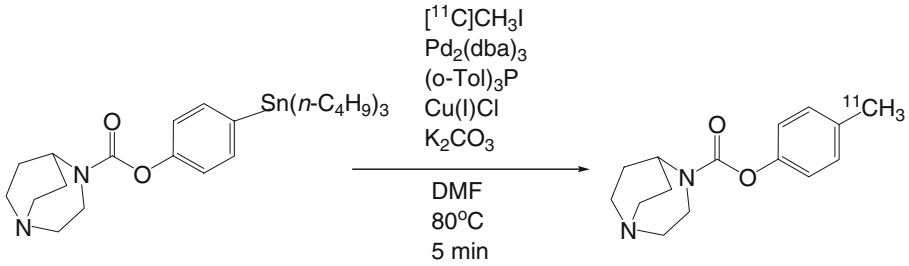

Fig. 1 Radiosynthesis of [^{11}C]CHIBA-1001

dipalladium(0) (2.8 mg, 3.0 μmol). The [^{11}C]methyl iodide produced was trapped in the reaction mixture of DMF (0.25 ml) with air cooling. The reaction mixture was heated at 80°C for 5 min. After adding 1.4 ml of high-performance liquid chromatography (HPLC) eluent [acetonitrile/50 mM acetic acid/50 mM ammonium acetate, (25/37.5/37.5, v/v/v)], the reaction mixture was passed through the Fine Filter F (Forte Grow Medical Co. Ltd, Tochigi, Japan) equipped with glass fiber wool and followed by injection onto the preparative HPLC: YMC-Pack Pro C18 RS S-5 μm [10 mm inner diameter (i.d.) × 250 mm length, YMC, Kyoto, Japan] with a mobile phase of acetonitrile/50 mM acetic acid/50 mM ammonium acetate (25/37.5/37.5, v/v/v) at a flow rate of 5.0 ml/min (UV detector at 260 nm). The retention time (RT) of [^{11}C]CHIBA-1001 was 8 min. The fraction of [^{11}C]CHIBA-1001 was collected in a flask containing 0.1 ml of 250 mg/ml ascorbate injection and evaporated to dryness. The residue was dissolved in physiological saline, and the solution was filtered through a 0.22-μm membrane filter (Millex GV, Nihon Millipore Ltd, Tokyo, Japan). Radiochemical purity was analyzed by HPLC using a TSKgel super-ODS column (4.6 mm i.d. × 100 mm length, Toso, Tokyo, Japan) with a mobile phase of acetonitrile/50 mM acetic acid/50 mM ammonium acetate (20/40/40, v/v/v) at a flow rate of 1.0 ml/min (UV detector at 220 nm). The RT of [^{11}C]CHIBA-1001 was 4.6 min. To determine specific activity, the mass (mmol) of the radioligand with a known radioactivity (TBq) was determined by an HPLC comparison of UV absorbance at 220 nm of the radioligand with those of known concentrations of the corresponding nonradioactive ligand.

Analysis of total tin residues

The determination of tin residues in the product fraction was performed according to the US Environmental Protection Agency document 3015A (EPA3015A: Microwave Assisted Acid Digestion of Aqueous Samples and Extracts. In: *Test methods for evaluating solid waste, physical/chemical methods*. SW-846 On-line, http://www.epa.gov/epaoswer/hazwaste/test/sw846.htm). Briefly, aqueous samples were extracted with concentrated nitric acid, using microwave heating by an ETHOS-TC microwave unit (Milestone Inc., Shelton, CT). A sample and nitric acid (2 ml) were placed in a tetrafluoromethane (TFM) vessel. The vessel was sealed and heated in the microwave unit at 230°C for 30 min. After cooling, the vessel contents were diluted to 20 ml with ultrapure water. The sample solutions were analyzed by the inductively coupled plasma mass spectrometer (ICP-MS) (ICPM-8500, Shimadzu Co., Kyoto, Japan). The isotopic masses used were Rh (internal standard) (103 m/z) and Sn (118 m/z). The detection limit is about 10 μg/l.

Tissue distribution in mice

[^{11}C]CHIBA-1001 (9.2 MBq/46 pmol) was intravenously injected into mice (male 8 weeks old). The mice were killed by cervical dislocation 1, 5, 15, 30, 60, and 90 min after injection ($n = 4$). The blood was collected by heart puncture, and the tissues were harvested. The samples were measured for ^{11}C-radioactivity with an auto-gamma counter (Wallac, Turk, Finland) and weighed. The tissue uptake of ^{11}C was expressed as a percentage of the injected dose per organ (%ID/organ) or a percentage of the injected dose per gram of tissue (%ID/g). The tissue distribution data were extrapolated to the adult male phantom using the % kg/g method [20], and radiation absorbed dose and effective dose for human adults were estimated using the software OLINDA/EXM (Vanderbilt University, Nashville, TN, USA) [21].

Acute toxicity

Toxicity studies of CHIBA-1001 were performed at the Mitsubishi Chemical Safety Institute Ltd (Tokyo, Japan). Acute toxicity was assayed in Crj:CD(SD)IGS rats (SPF). CHIBA-1001 at a dose of 3.20 mg/kg body weight (0.32 mg/ml in physiological) was injected intravenously into 5-week-old rats weighing 152–179 and 125–145 g, for males ($n = 5$) and females ($n = 5$), respectively. The dose of 3.20 mg/kg body weight is the 41,000-fold equivalent of the postulated administration dose (0.078 μg/kg body weight) of 500 MBq [^{11}C]CHIBA-1001, with a specific activity of 37 TBq/mmol for humans weighing 60 kg. The

three lots of [^{11}C]CHIBA-1001 prepared above were also assayed after the decay-out of ^{11}C. Each of the two [^{11}C]CHIBA-1001 preparations was injected intravenously into 5-week-old male and female rats ($n = 3$ for each) at doses of 1.63 μg/2.94 ml/kg body weight and 2.46 μg/2.66 ml/kg body weight, equivalent to 150-fold the postulated administration dose of 500 MBq [^{11}C]CHIBA-1001 for humans. One lot (4.11 μg/3.27 ml/kg body weight), which was equivalent to 300-fold the postulated administration dose, was also injected into 5-week-old male and female rats ($n = 3$ for each). They were observed four times (0.5, 1, 3, and 6 h after the injection) at day 1 and thereafter once daily for clinical signs until 15 days, and weighed on days 4, 8, and 15. At the end of the 15-day observation period, the rats were euthanized and a macroscopic analysis was performed.

Ames test

Mutagenicity tests were performed at the Mitsubishi Chemical Safety Institute Ltd (Tokyo, Japan). CHIBA-1001 was tested for mutagenicity using the Ames test with four histidine-requiring strains of *Salmonella typhimurium* (TA98, TA100, T1535, and T1537) with and without the S9 mixture at a dose range of 0.0391–5,000 μg/plate by the standard method.

Metabolite study in mice

[^{11}C]CHIBA-1001 (50–167 MBq/1.1–2.6 nmol) was intravenously injected into mice (8–10 weeks old, 35–40 g), and 15 ($n = 4$) and 30 ($n = 3$) min later they were killed by cervical dislocation. Blood was removed by heart puncture using a heparinized syringe, and the brain was removed. The blood was centrifuged at 7,000×g for 1 min at 4°C to obtain the plasma, which was denatured with a third volume of 20% trichloroacetic acid (TCA) in acetonitrile in an ice-water bath. The suspension of plasma was centrifuged in the same condition and divided into acid-soluble and acid-precipitable fractions. The precipitate was re-suspended in 0.5 ml of 10% TCA in acetonitrile followed by centrifugation. This procedure was repeated twice. The cerebral cortex (20–50 mg) was homogenized in 1 ml of 20% TCA in acetonitrile/water (1/1, v/v). The homogenate was treated as described above. Radioactivity in the three acid-soluble fractions and precipitates was measured with an auto-gamma counter. In this treatment of plasma and brain tissues, <1% of the total radioactivity was left in the final precipitates. The acid-soluble fractions were combined and diluted with two volumes of 50 mM sodium acetate, pH 4.5. After centrifugation of the samples as described above, the supernatant was analyzed by HPLC with a radioactivity detector (FLO-ONE 150TR, Packard Instrument, Meriden, CT). A Nova-Pak C18 column equipped in an RCM 8 × 10 module (8 mm × 100 mm, Waters, Milford, MA) was used with acetonitrile/50 mM acetic acid/50 mM sodium acetate, pH 4.5 (25/37.5/37.5, v/v) at a flow rate of 2 ml/min. The elution profile was monitored with a radioactivity detector. The RT of [^{11}C]CHIBA-1001 was 6.3 min. The recovery in the eluate of the injected radioactivity was essentially quantitative.

Clinical study

A clinically normal male subject (48 years old, 60.7 kg) participated in this study, and written informed consent was obtained from him. He did not show any abnormality in the brain magnetic resonance imaging (MRI) scan. The PET camera used was a SET-2400W (Shimadzu Co., Kyoto, Japan), which has an axial field-of-view of 20 cm and acquires 63 slices at a center-to-center interval of 3.125 mm [22]. After transmission scanning with a rotating [^{68}Ga]/[^{68}Ge] line source to correct for attenuation, [^{11}C]CHIBA-1001 (680 MBq/17 nmol) was injected intravenously for 2 min into the subject, and PET scanning was performed for 90 min in two-dimensional mode (10 s × 6 frames, 30 s × 3 frames, 60 s × 5 frames, 150 s × 5 frames, and 300 s × 14 frames). Arterial blood was taken at 10, 20, 30, 40, 50, 60, 70, 80, 90, 100, 110, 120, 145, 160, 175, and 180 s, as well as at 5, 7, 10, 15, 20, 30, 40, 50, 60, and 90 min, and the whole blood and plasma radioactivity was measured and expressed as a standardized uptake value [SUV, (activity/g blood or plasma)/(injected activity/g body weight)]. After the PET scan, urine was recovered from the subject 120 min after injection of the tracer, and the radioactivity was then measured.

Metabolites of [^{11}C]CHIBA-1001 in the plasma sampled at 3, 10, 20, 30, 40, and 60 min and in urine recovered at 120 min were analyzed by HPLC as described above. In the case of urine, the sample was directly applied to HPLC.

Tomographic images were reconstructed using a filtered back projection method with a cut-off frequency of 1.25 cycle/cm and order 2. The data were collected in a 128 × 128 × 31 matrix, and the voxel size was 2 × 2 × 6.25 mm. Regions of interest (ROIs) were placed on the frontal, temporal, parietal, and occipital cortices, the head of the caudate nucleus, and the putamen, thalamus, amygdala, hippocampus, and cerebellum with reference to the coregistered MRI. Time–activity curves (TACs) for these ROIs were calculated as Bq/ml or as an SUV, (activity/ml tissue)/(injected activity/g body weight). Using the TACs of tissues and the metabolite-corrected TAC of plasma, the total distribution volume (V_T) for [^{11}C]CHIBA-1001 was evaluated by Logan graphical analysis [23].

Results

Radiosynthesis

[^{11}C]CHIBA-1001 was synthesized by methylation of the tributylstannyl precursor with [^{11}C]CH_3I in a palladium-promoted Stille cross-coupling reaction. The synthesis was conducted by a one-pot procedure. A preparative HPLC chromatogram showed that usually over 80% of a reaction mixture's radioactivity was derived from [^{11}C]CHIBA-1001 (RT = 8 min) and the residues were from radiolabeled by-products (RT = 2.9, 4.3, and 7.5 min). The total synthesis time was within 30 min from the end of bombardment. The decay-corrected radiochemical yields of [^{11}C]CHIBA-1001 based on [^{11}C]CH_3I were 67.2 ± 7.6% (range 56.0–83.8) (n = 10). The radiochemical purity of [^{11}C]CHIBA-1001 was always greater than 99%. It gradually decreased with time but remained >99% for at least 30 min after the preparation in the presence of ascorbate. The specific activities of [^{11}C]CHIBA-1001 were 54.8 ± 8.7 TBq/mmol (range 41.3–66.8), at 30 min before the end of irradiation (n = 10). The considerably toxic tri(*o*-tolyl)phosphine and tributylstannyl iodide were not eluted from the HPLC column with the mobile phase used, when [^{11}C]CHIBA-1001 purification was performed. Finally, the sterility and apyrogenicity of the products were confirmed.

The three lots of product solution were analyzed for tin residues using inductively coupled plasma mass spectrometry. Contamination of tin in the final product was under detectable range (<10 μg/L). The amount of tin was below the LD_{50} for tri-*n*-butyltin, which was reported to be 10 mg/kg for acute toxicity [24].

Radiation dosimetry

The tissue distribution of the radioactivity after injection of [^{11}C]CHIBA-1001 into mice is summarized in Tables 1 and 2. The lung showed the highest initial uptake (%ID/g) followed by the kidneys, heart, pancreas, brain, small intestines, muscle, liver, and spleen. The level of radioactivity in the brain and spleen increased for the first 5 min and then gradually decreased. The levels in the lungs, kidneys, heart, muscle, and blood gradually decreased, whereas those in the pancreas and liver increased for 15 and 30 min, respectively, and then decreased. The level of radioactivity in the small intestines and testis increased for 15 and 30 min, respectively, and then maintained the same level. The levels in other tissues investigated were low. From these data, we estimated the radiation-absorbed doses (Table 3). The effective dose according to the risk-weighting factors of ICRP60 [25] was estimated at 3.8 μSv/MBq.

Acute toxicity

Acute toxicity was evaluated after a single intravenous administration of CHIBA-1001 at a dose of 3.20 mg/kg body weight and three lots of [^{11}C]CHIBA-1001 preparations in a dose range of 1.63–4.11 μg/kg. No mortality was found in the rats. All of the rat groups showed normal gains in body weight compared with that in the control animals, and no clinical signs were observed over a 15-day period. Also, no abnormality was found in their postmortem macroscopic examination.

Mutagenicity

When a bacterial reverse mutation test was conducted on the *S. thyphimurium* mutation test, no mutagenic activity was observed for CHIBA-1001.

Metabolite study in mice

HPLC analysis of plasma showed at least four labeled metabolites in addition to [^{11}C]CHIBA-1001 (RT 6.3 min). The RTs of two major metabolites were 2.6 and 5.6 min, and several minor metabolites were detected between 2.2 and 3.6 min. The former two metabolites were negligibly found in the brain. At 15 min after injection of [^{11}C]CHIBA-1001, the percentages of the unchanged form in the brain and plasma were 99.6 ± 0.2% (n = 3) and 43.6 ± 8.6% (n = 4), respectively, and the corresponding figures were 99.4 ± 0.5% and 21.3 ± 1.2% (n = 3) at 30 min after injection.

PET imaging of α7 nAChRs in the human brain

Figure 2 shows the magnetic resonance images (MRIs) of the corresponding slices (a), static images (b), and parametric brain images for the V_T (c) of [^{11}C]CHIBA-1001 in a healthy human subject. The tracer was widely distributed in all brain regions. Figure 3 shows the TACs of [^{11}C]CHIBA-1001 in the ten brain regions, blood, and plasma after intravenous injection of [^{11}C]CHIBA-1001 into a human. Radioactivity in all the brain regions except for the hippocampus peaked at about 15 min after administration of [^{11}C]CHIBA-1001, whereas radioactivity in the hippocampus peaked at about 30 min after administration. Plasma radioactivity rapidly decreased after a bolus injection. The concentrations of radioactivity and the overall shapes of the TACs in blood and plasma were well matched. The rank order of V_T values was the thalamus (21.6), amygdale (20.3), putamen (20.0), hippocampus (19.7), temporal (18.9), frontal (18.1), and parietal (17.2) cortices, head of the caudate nucleus (17.2), and cerebellum (16.8), and occipital cortex (16.6).

Table 1 Tissue distribution of radioactivity in mice after intravenous injection of [^{11}C]CHIBA-1001

	Injection dose/g tissue (%)[a]					
	1 min	5 min	15 min	30 min	60 min	90 min
Blood	1.22 ± 0.20	0.65 ± 0.13	0.55 ± 0.05	0.71 ± 0.08	0.70 ± 0.09	0.52 ± 0.01
Brain	4.57 ± 0.82	5.83 ± 1.27	5.16 ± 0.58	2.93 ± 0.22	1.63 ± 0.13	1.21 ± 0.30
Heart	6.16 ± 1.00	2.17 ± 0.44	1.13 ± 0.10	0.93 ± 0.08	0.67 ± 0.16	0.58 ± 0.04
Lung	23.77 ± 5.11	10.59 ± 1.19	5.86 ± 0.69	3.54 ± 0.39	2.00 ± 0.07	1.44 ± 0.30
Liver	2.34 ± 0.64	4.67 ± 1.32	12.74 ± 2.16	17.32 ± 2.06	15.81 ± 1.30	11.21 ± 1.70
Spleen	2.32 ± 0.35	5.44 ± 0.76	4.78 ± 0.46	3.25 ± 0.44	1.78 ± 0.20	1.14 ± 0.19
Pancreas	5.54 ± 1.04	8.55 ± 1.61	9.15 ± 0.53	6.49 ± 0.70	3.46 ± 0.27	2.34 ± 0.37
Stomach	1.82 ± 0.14	3.25 ± 0.89	3.32 ± 0.82	2.51 ± 0.51	1.69 ± 0.49	2.43 ± 0.52
Small intestine	3.00 ± 0.41	4.08 ± 0.71	4.23 ± 0.47	4.11 ± 0.40	3.96 ± 0.30	5.77 ± 0.50
Large intestine	1.48 ± 0.11	2.13 ± 0.36	2.58 ± 0.33	2.04 ± 0.30	1.36 ± 0.34	1.40 ± 0.20
Kidney	13.17 ± 2.44	8.67 ± 1.93	4.96 ± 0.45	3.40 ± 0.28	3.40 ± 1.16	2.22 ± 0.30
Testis	1.02 ± 0.17	1.66 ± 0.37	2.67 ± 0.47	3.30 ± 0.16	2.94 ± 0.70	3.22 ± 0.90
Bone	1.69 ± 0.10	1.32 ± 0.25	1.42 ± 0.08	0.79 ± 0.15	0.54 ± 0.08	1.20 ± 0.14
Muscle	2.46 ± 0.76	1.51 ± 0.28	0.99 ± 0.11	0.69 ± 0.06	0.54 ± 0.07	0.43 ± 0.04

[a] Mean ± SD ($n = 4$)

Table 2 Organ distribution of radioactivity in mice after intravenous injection of [^{11}C]CHIBA-1001

	Injection dose/organ (%)[a]					
	1 min	5 min	15 min	30 min	60 min	90 min
Brain	2.16 ± 0.47	2.60 ± 0.64	2.24 ± 0.36	1.29 ± 0.15	0.70 ± 0.07	0.60 ± 0.16
Heart	0.76 ± 0.10	0.33 ± 0.03	0.17 ± 0.04	0.14 ± 0.02	0.10 ± 0.03	0.07 ± 0.05
Lung	5.18 ± 1.39	2.44 ± 0.28	1.27 ± 0.22	0.69 ± 0.05	0.42 ± 0.04	0.31 ± 0.06
Liver	3.93 ± 1.37	8.82 ± 2.17	23.93 ± 1.17	30.05 ± 4.77	24.06 ± 1.74	19.12 ± 4.09
Spleen	0.26 ± 0.04	0.73 ± 0.13	0.64 ± 0.04	0.37 ± 0.08	0.20 ± 0.03	0.12 ± 0.04
Pancreas	1.23 ± 0.43	1.71 ± 0.65	1.73 ± 0.21	1.15 ± 0.22	0.65 ± 0.15	0.45 ± 0.08
Stomach	0.97 ± 0.23	1.86 ± 0.58	1.79 ± 0.40	1.48 ± 0.22	0.96 ± 0.19	0.89 ± 0.07
Small intestine	4.82 ± 1.03	7.26 ± 1.83	7.17 ± 0.91	6.53 ± 0.68	6.94 ± 0.94	7.95 ± 0.52
Large intestine	1.30 ± 0.19	2.39 ± 0.54	2.47 ± 0.39	1.91 ± 0.27	1.44 ± 0.18	1.35 ± 0.21
Kidney	6.69 ± 1.12	4.82 ± 0.95	2.58 ± 0.42	1.71 ± 0.16	1.71 ± 0.71	1.22 ± 0.16
Testis	0.24 ± 0.05	0.40 ± 0.11	0.68 ± 0.11	0.77 ± 0.04	0.67 ± 0.09	0.69 ± 0.18
Bladder	0.05 ± 0.01	0.09 ± 0.06	0.16 ± 0.17	0.15 ± 0.03	0.48 ± 0.31	0.84 ± 0.52
Urine		0.06 ± 0.08	2.85 ± 0.65	9.63 ± 1.13	20.39 ± 5.11	28.74 ± 2.92

[a] Mean ± SD ($n = 4$)

HPLC analysis revealed that the percentages of the unchanged form of [^{11}C]CHIBA-1001 gradually decreased: 99.2, 98.5, 94.9, 92.2, 84.6, and 81.4%, at 3, 10, 20, 30, 40, and 60 min, respectively. In urine obtained 120 min post-injection, 3.9% of the total injected radioactivity was recovered. HPLC analysis of urine clearly showed at least four labeled metabolites of [^{11}C]CHIBA-1001, with retention times of 1.8, 3.0, 4.0, and 4.5 min, respectively. That of [^{11}C]CHIBA-1001 was 6.3 min, and 87.4% of the radioactivity in the urine was detected as [^{11}C]CHIBA-1001.

Discussion

In previous in vitro membrane-binding and in vivo non-human primate PET studies, we demonstrated that [^{11}C]CHIBA-1001 has the potential for mapping α7 nAChRs in the CNS as a PET ligand [18]. In this work, we investigated the dosimetry of [^{11}C]CHIBA-1001 and the acute toxicity and mutagenicity of CHIBA-1001 as a preclinical study. We also established the practical radiosynthesis method for clinical use, and finally performed the first PET imaging of the human brain.

Table 3 Absorbed dose of [^{11}C]CHIBA-1001 for human adults estimated from mouse data

	μGy/MBq		μGy/MBq
Brain	3.4	Upper large intestine wall	3.4
Thyroid	2.3	Lower large intestine wall	3.2
Thymus	2.3	Adrenals	3.0
Breasts	2.1	Kidneys	4.9
Heart wall	2.6	Testes	2.6
Lungs	5.1	Ovaries	2.8
Liver	10.1	Uterus	3.1
Gall bladder wall	3.6	Urinary bladder wall	10.8
Pancreas	5.8	Osteogenic cells	4.2
Spleen	3.5	Red marrow	2.5
Stomach wall	3.4	Muscle	1.8
Small intestine	4.0	Skin	1.8
Remainder of body	2.8 μGy/MBq		

Effective dose 3.8 μSv/MBq

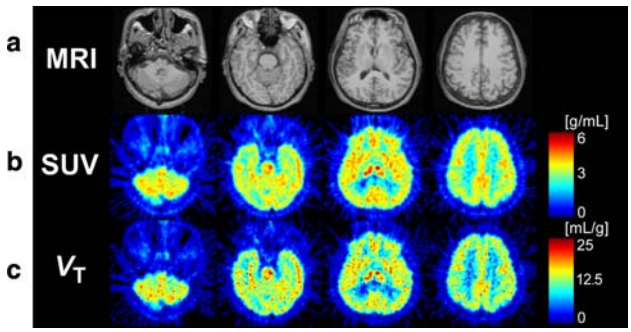

Fig. 2 PET images of human brain with [^{11}C]CHIBA-1001. **a** Magnetic resonance images (MRI) of the corresponding slices. **b** Static images acquired from 0 to 90 min after injection of [^{11}C]CHIBA-1001 expressed as SUV. **c** A parametric image for the total distribution volume of [^{11}C]CHIBA-1001 generated using Logan graphical analysis. The data from 30 to 90 min were applied to the Logan plot analysis

The palladium-mediated reaction of stannanes with [^{11}C]CH_3I employing Stille cross-coupling reactions was applied to various PET ligand syntheses [26]. This strategy was successfully employed in the radiosynthesis of [^{11}C]CHIBA-1001. In this study, we optimized the method for synthesizing [^{11}C]CHIBA-1001. The reaction mixtures must be prepared immediately before the end of irradiation and added to a reaction vial as soon as possible. Under these conditions, the [^{11}C]methylation of the precursor was reproducible and selective (>80% of radioactivity was from [^{11}C]CHIBA-1001). However, when reaction mixtures were prepared more than 5 min before the end of irradiation, the radiolabeled by-products (RT = 2.9 and

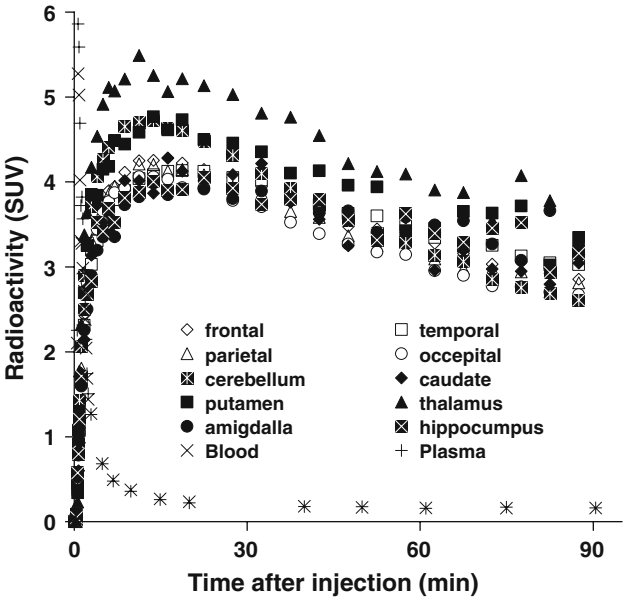

Fig. 3 Time–activity curves of the ten brain regions and of blood and plasma after intravenous injection of [^{11}C]CHIBA-1001 into a human. The radioactivity levels are expressed as the SUV

4.3 min) were increased and radiochemical yields were significantly decreased (data not shown).

Also of concern is that the Stille cross-coupling reactions produce toxic tin-containing contaminants. This may limit the application of the Stille cross-coupling, especially when PET ligand synthesis is used clinically. Therefore, in this study, we evaluated total tin residues in the final product by using the ICP-MS method. The ICP-MS analysis showed that contamination of tin in the final product was under detectable range (<10 μg/L). Moreover, final products do not include the starting materials-tri(*o*-tolyl)phosphine and tributylstanyl iodide—because these materials were not eluted from the HPLC column with the mobile phase used when [^{11}C]CHIBA-1001 was purified. Radiochemical purity and specific activity were satisfactory, and the sterility and apyrogenicity of the products were confirmed. Gathering these quality control data, we considered that [^{11}C]CHIBA-1001 has sufficient quality for clinical usage. The radiation-absorbed dose was slightly higher in the liver and urinary bladder walls than in other organs studied, but was nonetheless low enough for clinical use. The absence of any abnormality in rats in the acute toxicity test and the absence of mutagenicity of CHIBA-1001 together demonstrate the clinical suitability of [^{11}C]CHIBA-1001 in PET studies for humans.

As C–C bond is generally believed to be metabolically more stable than carbon-hetero atom bond, a carbon-11 labeled radiopharmaceutical prepared by Stille cross-coupling reaction has more possibility to give lipophilic metabolites than ordinal ^{11}C-methylation. Therefore, we

examined whether labeled metabolites exist within brain tissue or not. In the metabolite study in mice, a major lipophilic metabolite with the retention time of 5.6 min was detected in plasma, while it was negligible in the brain tissues (<0.6% at 30 min after injection). The HPLC profile of the metabolites in the human plasma in this study corresponded well to that of the mice except the most lipophilic metabolite with 5.6 min of retention. However, in another patient, small amount of the lipophilic metabolite with 5.6 min of retention in the plasma was observed (data not shown). From the above results, these plasma metabolites could not hamper the quantitative analysis of brain uptake of [^{11}C]CHIBA-1001.

In the human brain, [^{11}C]CHIBA-1001 was widely distributed in all brain regions. V_T values ranged from 16.6 to 21.6. The regional distribution pattern of [^{11}C]CHIBA-1001 is consistent with that expected in vitro [8, 10, 11, 27, 28], but different from that of $\alpha4\beta2$ nAChRs [28]. However, it is slightly different from the regional distribution in the monkey brain [18]. In the human brain, remarkable radioactivity accumulation was observed in the cerebellum. A human postmortem brain study showed that [^{125}I]α-bungarotoxin binding in the cerebellum was of the same level as that of the cortex [7, 8]. In the monkey brain, the $\alpha7$ mRNA expression pattern resembled that of postmortem human brain [6, 7]. However, it is important to recognize that discrepancies between protein and mRNA expression will occur several times. In addition, PET images were the mean values of high and low densities of the binding sites, which resulted in the apparent discrepancy between the in vitro findings such as autoradiography (ARG) and the PET images. Especially, the partial volume effect based on the spatial resolution may be considered in the PET study. The differences in results may be methodological, such as species, ARG, or PET camera resolution.

The receptor-specific binding of [^{11}C]CHIBA-1001 was not confirmed in this preliminary study. Therefore, a further receptor blocking study using selective $\alpha7$ nAChR antagonists/agonists is currently under way.

The concentrations of radioactivity and the overall shapes of the TACs in blood and plasma were well matched. This result might indicate that [^{11}C]CHIBA-1001 does not bind or incorporate into the cellular components of the blood. A species difference between human and non-human primate was also found in the peripheral metabolism of [^{11}C]CHIBA-1001. The finding that [^{11}C]CHIBA-1001 was much more stable peripherally in a human than in monkeys is a good property as a PET ligand: the percentages of intact form in the plasma of human and monkeys were >80% and <60% at 60 min post-injection, respectively [18].

Studies of postmortem human brain samples demonstrated that $\alpha7$ nAChRs are less dense in the brain of patients with Alzheimer's disease (AD), dementia with Lewy bodies (DLB), and schizophrenia [10–12]. In AD patients, there are significant declines in [^{125}I]α-bungarotoxin binding sites in the reticular nucleus [10]. An extensive reduction (50%) in [^{125}I]α-bungarotoxin binding sites in the reticular nucleus was observed in DLB patients [11]. Schizophrenic patients have a small but significant decrease in [^{125}I]α-bungarotoxin binding sites in the hippocampus [12]. Therefore, it would be of great interest to determine, using [^{11}C]CHIBA-1001 and PET, whether or not $\alpha7$ nAChRs are altered in the intact brain of patients with these diseases.

In conclusion, these findings suggest that [^{11}C]CHIBA-1001 is a suitable radioligand for imaging $\alpha7$ nAChRs in the human brain, as it offers acceptable dosimetry and pharmacological safety at the dose required for adequate PET imaging.

Acknowledgments This work was supported by grant from the Program for Promotion of Fundamental Studies in Health Sciences of the National Institute of Biomedical Innovation of Japan (Grant ID: 06-46, to K.·Hashimoto and K. Ishiwata). We thank Mr. Kunpei Hayashi and Ms. Hiroko Tsukinari for technical assistance.

References

1. Lukas RJ, Changeux JP, Le Novere N, Albuquerque EX, Balfour DJ, Barg DK, et al. International Union of Pharmacology. XX. Current status of the nomenclature for nicotinic acetylcholine receptors and their subunits. Pharmacol Rev. 1999;51:397–401.
2. Paterson D, Nordberg A. Neuronal nicotinic receptors in the human brain. Prog Neurobiol. 2000;61:75–111.
3. Romanelli MN, Gratteri P, Guandalini L, Martini E, Bonaccini C, Gualtieri F. Central nicotinic receptors: structure, function, ligands, and therapeutic potential. Chem Med Chem. 2007;2:746–67.
4. Davies AR, Hardick DJ, Blagbrough JS, Potter BV, Wolstenholme AJ, Wonnacott S. Characterization of the binding of [^{3}H]methyllycaconitine: a new radiologand for labeling $\alpha7$-type neuronal nicotinic acetylcholine receptors. Neuropharmacology. 1999;38:679–90.
5. Kulak JM, Schneider JS. Differences in $\alpha7$ nicotinic acetylcholine receptor binding in mortor symptomatic and asymptomatic MPTP-treated monkeys. Brain Res. 2004;999:193–202.
6. Quik M, Polonskaya Y, Gillespie A, Jakowec M, Lloyd K, Langston W. Localization of nicotinic receptor subunit mRNAs in monkey brain by in situ hybridization. J Comp Neurol. 2000;425:58–69.
7. Breese CR, Adams C, Logel J, Drebing C, Rollins Y, Barnhart M, et al. Comparison of the regional expression of nicotinic acetylcholine receptor $\alpha7$ mRNA and [^{125}I]-α-bungarotoxin binding in human postmortem brain. J Comp Neurol. 1997;387:385–98.
8. Falk L, Nordberg A, Seiger Å, Kjældgaard A, Hellström-Lindahl E. Higher expression of $\alpha7$ nicotinic acetylcholine receptors in human fetal compared to adult brain. Dev Brain Res. 2003;142:151–60.
9. Berg DK, Conroy WG. Nicotinic $\alpha7$ receptors: synaptic options and down stream signaling in neurons. J Neurobiol. 2002;53:512–23.
10. Court J, Martin-Ruiz C, Piggott M, Spurden D, Griffiths M, Perry E. Nicotinic receptor abnormalities in Alzheimer's disease. Biol Psychiatry. 2001;49:175–84.

11. Court J, Spurden D, Lloyd S, McKeith I, Ballard C, Cairns N, et al. Neuronal nicotinic receptors in dementia with Lewy bodies and schizophrenia: α-bungarotoxin and nicotinic binding in thalamus. J Neurochem. 1999;73:1590–7.
12. Freedman R, Hall M, Alder LE, Leonard S. Evidence in post-mortem brain tissue for decreased numbers of hippocampal nicotinic receptors in schizophrenia. Biol Psychiatry. 1995;38: 22–33.
13. Wang HY, Lee DH, D'Andrea MR, Peterson PA, Shank RP, Reitz AB. Beta-Amyloid (1–42) binds to α7 nicotinic acetylcholine receptor with high affinity. Implications for Alzheimer's disease pathology. J Biol Chem. 2000;275:5626–32.
14. Hashimoto K, Koike K, Shimizu E, Iyo M. α7 Nicotinic receptor agonists as potential therapeutic drugs for schizophrenia. Curr Med Chem CNS Agents. 2005;5:171–84.
15. Dolle F, Valette H, Hinnen F, Vaufrey F, Demphel S, Coulon C, et al. Synthesis and preliminary evaluation of a carbon-11-labelled agonist of the α7 nicotinic acetylcholine receptor. J Labelled Cpd Radiopharm. 2001;44:785–95.
16. Pomper MG, Phillips E, Fan H, McCarthy DJ, Keith RA, Gordon JC, et al. Synthesis and biodistribution on radiolabeled α7 nicotinic acetylcholine receptor ligands. J Nucl Med. 2005;46: 326–34.
17. Ogawa M, Tatsumi R, Fujio M, Katayama J, Magata Y. Synthesis and evaluation of [^{125}I]I-TSA as a brain nicotinic acetylcholine receptor α7 subtype imaging agent. Nucl Med Biol. 2006;33: 311–36.
18. Hashimoto K, Nishiyama S, Ohba H, Matsuo M, Kobashi T, Takahagi M, et al. [^{11}C]CHIBA-1001 as a novel PET ligand for α7 nicotinic receptors in the brain: a PET study in conscious monkeys. PLoS ONE. 2008;3:e3231.
19. Kawamura K, Shiba K, Tsukada H, Nishiyama S, Mori H, Ishiwata K. Synthesis and evaluation of vesamicol analog (−)-*o*-[^{11}C]methylvesamicol as a PET ligand for vesicular acetylcholine transporter. Ann Nucl Med. 2006;20:417–24.
20. Kirschner AS, Ice RD, Beierwaltes WH. Radiation dosimetry of 131I-19-iodocholesterol: the pitfalls of using tissue concentration data—reply. J Nucl Med. 1975;16:248–9.
21. Stabin MG, Sparks RB, Crowe E. OLINDA/EXM: the second-generation personal computer software for internal dose assessment in nuclear medicine. J Nucl Med. 2005;46:1023–7.
22. Fujiwara T, Watanuki S, Yamamoto S, Miyake M, Seo S, Itoh M, et al. Performance evaluation of a large axial field-of-view PET scanner: SET-2400W. Ann Nucl Med. 1997;11:307–13.
23. Logan J, Fowler JS, Volkow ND, Wolf AP, Dewey SL, Schlyer DJ, et al. Graphical analysis of reversible radioligand binding from time–activity measurements applied to [*N*-^{11}C-methyl]-(−)-cocaine PET studies in human subjects. J Cereb Blood Flow Metab. 1990;19:615–23.
24. Stoner HB, Barnes JM, Duff JI. Studies on the toxicity of alkyl tin compounds. Br J Pharmacol. 1955;10:16–25.
25. International Commission on Radiological Protection. Recommendation of the International Commission on Radiological Protection: Publication 60. Oxford: Pergamon Press; 1990. p. 4–11.
26. Wuest F, Berdt M, Kniess T. Carbon-11 labeling chemistry based upon [^{11}C]methyl iodide. In: Schubiger PA, Lehman L, Fribe M, editors. PET chemistry. The driving force in molecular imaging. Berlin: Springer; 2007. p. 183–213.
27. Marutle A, Zhang X, Court J, Piggott M, Johnson M, Perry R, et al. Laminar distribution of nicotinic receptor subtypes in cortical regions in schizophrenia. J Chem Neuroanat. 2001;22: 115–26.
28. Clementi GC. Neuronal nicotinic receptors: from structure to pathology. Prog Neurobiol. 2004;74:363–96.